
Provable Guarantees against Data Poisoning Using Self-Expansion and Compatibility

Charles Jin¹ Melinda Sun¹ Martin Rinard¹

Abstract

A recent line of work has shown that deep networks are highly susceptible to backdoor data poisoning attacks. Specifically, by injecting a small amount of malicious data into the training distribution, an adversary gains the ability to control the model’s behavior during inference. In this work, we propose an iterative training procedure for removing poisoned data from the training set. Our approach consists of two steps. We first train an ensemble of weak learners to automatically discover distinct subpopulations in the training set. We then leverage a boosting framework to recover the clean data. Empirically, our method successfully defends against several state-of-the-art backdoor attacks, including both clean and dirty label attacks. We also present results from an independent third-party evaluation including a recent *adaptive* poisoning adversary. The results indicate our approach is competitive with existing defenses against backdoor attacks on deep neural networks, and significantly outperforms the state-of-the-art in several scenarios.

1. Overview

The past few years has seen the rapid adoption of deep learning in real world applications, from digital personal assistants to autonomous vehicles. This trend shows no sign of abating, given the remarkable ability of deep neural networks to achieve (super)human performance on tasks such as computer vision (He et al., 2016), speed recognition (Graves et al., 2013), and game playing (Silver et al., 2016).

However, this widespread integration of deep networks presents a potential security risk, particularly in performance- and safety-critical applications. In this work, we focus on defending against *backdoor attacks* (Chen et al., 2017; Adi et al., 2018). Specifically, it has been demon-

strated that deep networks can be attacked by injecting small amounts of malicious data during training to create a backdoor in the model; once installed, an adversary can exploit the backdoor to arbitrarily control the network’s behavior at inference time. For instance, Gu et al. (2019) demonstrate a backdoor that causes a model to misclassify stop signs as speed signs by applying a (physical) sticker. These attacks are particularly pernicious in that the accuracy of the model on unperturbed data is generally not affected by the backdoor, thus making it difficult to identify models that have been compromised over the course of standard operation.

Techniques Inspired by the work of Balcan et al. (2005), we first introduce the notion of **self-expanding sets**, which is a bootstrapped measure of how well a set generalizes to itself. Under certain compatibility assumptions, we show that the process of identifying self-expanding sets naturally separates a dataset into a collection of homogeneous components (i.e., completely clean or completely poisoned). Given such a collection, we then provide a method to identify the clean distribution by boosting an ensemble of weak learners over the components.

To solve the key challenge of identifying self-expanding sets, we next propose the **Inverse Self-Paced Learning** algorithm. Our approach is based on vanilla self-paced learning, but uses quantile statistics instead of an absolute loss threshold, and also incrementally decreases, rather than increases, the size of the training set. We additionally prove sufficient conditions for the convergence of the algorithm.

Experimental Evaluation We implement the proposed Inverse Self-Paced Learning algorithm within our boosting framework, and evaluate its performance on two different backdoor attacks on CIFAR-10 (Krizhevsky, 2009). Our method completely defends against the attacks in almost every setting, and substantially reduces the success rate of the attack in the remaining cases. We also submitted our approach to a third party for evaluation on the GTSRB dataset (Houben et al., 2013) for traffic sign classification. The results show that our method is additional robust again a strong *adaptive* data poisoning adversary, which was previously shown to break three existing state-of-the-art defenses. Furthermore, all our results are achieved with minimal tun-

¹CSAIL, MIT, Cambridge, MA, USA. Correspondence to: Charles Jin <ccj@csail.mit.edu>.

ing to the expected amount of poison in the dataset, while reducing the accuracy on clean data by only 2-3%. Our approach thus presents a novel, empirically verified method for defending against backdoor attacks.

2. Related Work

Our separation results can be viewed as a clustering problem, where we exploit weak supervision in the form of class labels, related via our notions of self-expansion and compatibility. Many prior works analyze similar assumptions for weak or semi-supervised learning based on clustering (Seeger, 2000; Rigollet, 2007; Singh et al., 2008) or expansion (Wei et al., 2020). In general, these works define expansion as an intrinsic property of the input data, rather than with respect to a (weak) learner as we do. Perhaps the closest idea is found in co-training with expansion, introduced by (Balcan et al., 2005). They show that under a similar expansion assumption, learners fit independently to two different “views” of the data can supervise each other to improve their joint performance. However, a major departure from these prior works is that we do not use an expansion assumption to leverage a small set of trusted or confident labels for minimizing a global classification error, but rather use self-expansion to identify homogeneous components by fitting weak learners to certain local minima.

We also introduce the Inverse Self Paced Learning algorithm for efficiently finding self-expanding sets. Self paced learning (SPL) was introduced by Kumar et al. as an type of curriculum learning (Bengio et al., 2009), originally inspired by the observation that humans learn more efficiently from a curriculum, rather than examples presented in random order. SPL is a heuristic that dynamically creates a curriculum based on the losses of the model after each epoch, so as to incorporate the easier samples first. SPL and its variants have been observed to be resilient to noise both in theory (Meng et al., 2016) and practice (Jiang et al., 2018; Zhang et al., 2020), though prior works focus mostly on clean accuracy under unrealizable label noise; in contrast, we measure targeted misclassification accuracy under adversarially selected, realizable noise distributions.

Finally, several prior works propose methods for defending against backdoor attacks on neural networks. In general, it has been observed that standard techniques from robust statistics applied directly to the data does not suffice for identifying the poison (Tran et al., 2018); thus the standard approach is to first fit a deep network to the poisoned distribution, then apply techniques to the learned representations in the network layers. The Activation Clustering defense (Chen et al., 2018) uses dimensionality reduction followed by k-means clustering (k=2) on the activation patterns, and discards the smallest cluster. Tran et al. (2018) propose a Spectral Signature defense that removes the data with the

top ϵ eigenvalues, where ϵ is set to 1.5 times the amount of expected poison. Finally, Wang et al. (2019) propose the Neural Cleanse defense that first reverse-engineers a trigger by searching for patches that cause strong misclassification, then prunes neurons with large activations. While this general strategy suffices for nonadaptive data poisoning attacks, a recent work by Tan and Shokri (2020) shows that an adaptive adversary can exploit this dependence to successfully break all three defenses. In contrast, our approach differs significantly in that we do not use the activation patterns of a poisoned model, and an evaluation by an independent third party adversary showed that our defense remained successful against this attack (Section 6.3).

3. Background and Setting

We first establish some basic notation and assumptions about our classification setting. Let X be the input space, Y be the label space, and $L(\cdot, \cdot)$ be a loss function over $Y \times Y$. In this work, we assume a bounded loss function, which includes many commonly used loss functions such as the zero-one or cross entropy loss. Given a target distribution \mathcal{D} supported on $X \times Y$ and a parametric family of functions f_θ , the goal is to find the parameters θ that minimize the population risk $R(\theta) := \int_{X \times Y} L(f_\theta(x), y) dP_{\mathcal{D}}(x, y)$.

The learning problem (f_θ, \mathcal{D}) is realizable if (1) for every label y , the marginals $\mathcal{D}(\cdot|y)$ have disjoint support; and (2) there exist ground truth parameters θ^* with $R(\theta^*) = 0$. For simplicity, we assume a (possibly stochastic) learning algorithm \mathcal{A} that performs empirical risk minimization, i.e., given a set of samples T , \mathcal{A} tries to return θ minimizing $R_{emp}(\theta; T) := \sum_{i \in T} L(f_\theta(x_i), y_i)$. Clearly, given enough training samples $S = \{(x_1, y_1), \dots, (x_n, y_n)\}$ iid from \mathcal{D} , the empirical risk gets arbitrarily close to the population risk. We will identify the training set S with its indices $[n]$.

3.1. Data and threat model

We consider a mixture of n distributions $\{(\alpha_i, \mathcal{D}_i)\}_{i=1}^n$ such that $\mathcal{D} = \cup_i \{\mathcal{D}_i\}$ and $\sum_i \alpha_i = 1$. We observe N inputs according to the following two-step procedure:

$$d \sim \text{Cat}(\alpha_1, \dots, \alpha_n) \quad (1)$$

$$x, y \sim \mathcal{D}_d \quad (2)$$

where $\text{Cat}(\cdot)$ is a categorical random variable that returns i with probability α_i . If S is a set of samples produced by this process, for any subset $S' \subseteq S$, we will denote the samples drawn from the i^{th} distribution as S'_i , so that $S' = \cup_i S'_i$.

In this work, we are primarily concerned with the backdoor data poisoning model. It has been observed empirically that injecting a small amount of malicious data into the training

distribution effectively installs a backdoor in the model, whereby the behavior on clean data is otherwise unaffected, but an attacker can cause targeted misclassification during inference by overlaying a small trigger. In this case sampling from the training distribution is modeled as follows:

$$d \sim \text{Cat}(\alpha_1, \dots, \alpha_n) \quad (3)$$

$$x, y \sim \mathcal{D}_d \quad (4)$$

$$p \sim \text{Bern}(\rho) \quad (5)$$

$$x \leftarrow \tau(x), y \leftarrow \pi(y), \text{ if } p \quad (6)$$

where $\tau(\cdot)$ is the function which applies a small trigger, $\pi(\cdot)$ is a permutation on classes, and ρ controls the probability of observing a poisoned sample. Note that this procedure can easily be replicated within the original data model. We will also assume the attack is non-trivial in the sense that the perturbed source distributions $\tau(\mathcal{D}_i)$ and target distributions $\mathcal{D}_{\pi(i)}$ are disjoint for all i .

Given a model $f_\theta(\cdot)$, we measure the success of the attack using the *targeted misclassification risk*:

$$A_{emp}(\theta; T) := \sum_{i \in T} [f_\theta(x_i) = y_i \wedge f_\theta(\tau(x_i)) = \pi(y_i)] \quad (7)$$

In other words, the attack succeeds if, during inference, it can flip the label of a correctly-classified instance by applying the trigger $\tau(\cdot)$.

3.2. Learning objective

We formulate our learning objective in the more general data model. Without loss of generality, we assume the first p distributions are *primary distributions*, and the remaining $n - p$ are *noise distributions*. Given a training set S , we write $S_P = S_1 \cup \dots \cup S_p$ for the samples from the primary distributions, and $S_N = S_{p+1} \cup \dots \cup S_n$ for the samples from the noise distributions.

Our goal is to learn parameters $\tilde{\theta}$ which correspond to training only on the primary distributions: $\tilde{\theta} := \mathcal{A}(S_P)$. Note this objective differs significantly from simply minimizing the risk over the primary distributions when the mixed distribution \mathcal{D} is realizable, i.e., we are also interested in avoiding effects that occur on portions of the input space that have low density in the primary distributions. More explicitly, in terms of the data poisoning threat model (Equation 7), we note that training on $S_P \cup S_N$ would yield low risk over the unperturbed distributions, but also high targeted misclassification risk. Conversely, for sufficiently separated distributions $\tau(\mathcal{D}_i)$ and $\mathcal{D}_{\pi(i)}$, we expect that the hypothesis class f_θ enjoys low targeted misclassification risk when trained only on clean data.

4. Separation of Mixed Distributions

In this section, we introduce the main theoretical assumptions that allow us to separate the primary and noise distributions. Our main tool will be a property of “self-expanding” sets; intuitively, given a set, we resample at a given rate and measure how well the learning algorithm generalizes to the rest of the set. Under certain compatibility assumptions between the primary and noise components, we show that the set with the optimal expansion must be homogeneous, i.e., drawn entirely from either the primary or noise components. Finally, we fit weak learners to the recovered (homogeneous) sets in a simplified boosting framework to identify the primary component.

4.1. Self-expansion and compatibility

We begin by stating a formal characterization of the self-expanding property of sets:

Definition 4.1 (Self-expansion of sets.). *The α -expansion error of a set S , denoted $\epsilon(S; \alpha)$, is defined as*

$$\epsilon(S; \alpha) := |S|^{-1} \mathbb{E}[R_{emp}(\mathcal{A}(S'); S)] \quad (8)$$

where the expectation is over both the randomness in \mathcal{A} and S' , a random variable of $\alpha^{-1}|S|$ samples drawn from S with replacement.

This self-expansion property measures the ability of the learning algorithm \mathcal{A} to generalize to the empirical distribution of a set S ; intuitively, a smaller expansion error means that the set is both “easier” and “more homogeneous” with respect to the learning algorithm.

In what follows, we will assume that self-expansion satisfy the following convexity property:

Assumption 4.1 (Convexity of expansion). *$\epsilon(S; \alpha)$ is a convex decreasing function of α .*

The decreasing property rules out the existence of pathological sets where increasing the number of samples degrades performance; convexity holds when the expected marginal information gained from additional samples decreases as the number of samples increases.

We now use self-expansion to define a notion of compatibility between sets:

Definition 4.2 (Compatibility of sets.). *A (nonempty) set T is α -compatible with set S with margin $\delta \geq 0$ if*

$$\mathbb{E}[R_{emp}(\mathcal{A}(S' \cup T); S)] + \delta |S| \leq \mathbb{E}[R_{emp}(\mathcal{A}(S'); S)] \quad (9)$$

where the expectation is over the same random variables as in the definition of self-expansion. Furthermore, T is completely α -compatible with S if all (nonempty) subsets

$T' \subseteq T$ are α -compatible with S . Conversely, T is α -incompatible with S if the opposite holds, i.e.,

$$\mathbb{E}[R_{emp}(\mathcal{A}(S'); S)] + \delta|S| \leq \mathbb{E}[R_{emp}(\mathcal{A}(S' \cup T); S)] \quad (10)$$

(and similarly for complete incompatibility). We also say that strict compatibility (incompatibility) holds when $\delta > 0$.

In other words, T is compatible with S if adding T to the training set does not hurt generalization to S .

The following key assumption enables us to separate the primary and noise distributions. Intuitively, we want the primary and noise mixture components to be negatively correlated (or at least independent) in the sense that training on a noise distribution should not improve performance on a primary distribution, and vice versa:

Assumption 4.2 (Incompatibility of primary and noise distributions). *Let α be given. Then any pair of (nonempty) sets S_i and S_j drawn from \mathcal{D}_i and \mathcal{D}_j , respectively, are strictly and completely α -incompatible if $i \leq n$ and $j > n$ or $i > n$ and $j \leq n$.*

We are now ready to state the main result of this section. Given Assumption 4.2, we show that any subset of S which achieves the minimum expansion error consists entirely of data drawn from either the primary or noise distributions:

Lemma 4.1 (Sets minimizing expansion error are homogeneous.). *Let $S = S_1 \cup \dots \cup S_n$ be a set of samples drawn from a mixture of distributions $\{(\alpha_i, \mathcal{D}_i)\}_{i=1}^n$. Define*

$$S^* := \arg \min_{S' \subseteq S} \epsilon(S'; \alpha) \quad (11)$$

for some expansion factor α . Then if Assumption 4.2 holds for α , we have either that $S^* \subseteq S_P$ or $S^* \subseteq S_N$, where $S_P = S_1 \cup \dots \cup S_p$ and $S_N = S_{p+1} \cup \dots \cup S_n$.

Proof. We first prove a slightly more general result. Assume by way of contradiction that there exists a partition of S^* into two nonempty sets P and Q that are mutually strictly incompatible.

Let ϵ^* be the expansion error of S^* . By definition,

$$\mathbb{E}[R_{emp}(\mathcal{A}(S'); S)] = |S|\epsilon^* \quad (12)$$

where the expectation is taken over samples S' of size $\alpha^{-1}|S|$ drawn from S with replacement.

Given a fixed set of samples S' , we can write $Q' = S' \cap Q$

and $P' = S' \cap P$, and so

$$\begin{aligned} \mathbb{E}[R_{emp}(\mathcal{A}(S'); S)|S'] &= \mathbb{E}[R_{emp}(\mathcal{A}(S'); P)|S'] \\ &\quad + \mathbb{E}[R_{emp}(\mathcal{A}(S'); Q)|S'] \end{aligned} \quad (13)$$

$$\begin{aligned} &= \mathbb{E}[R_{emp}(\mathcal{A}(P' \cup Q'); P)|S'] \\ &\quad + \mathbb{E}[R_{emp}(\mathcal{A}(P' \cup Q'); Q)|S'] \end{aligned} \quad (14)$$

$$\begin{aligned} &> \mathbb{E}[R_{emp}(\mathcal{A}(P'); P)|S'] \\ &\quad + \mathbb{E}[R_{emp}(\mathcal{A}(Q'); Q)|S'] \end{aligned} \quad (15)$$

where the expectation is over the randomness in \mathcal{A} ; the first line follows from linearity of expectation, and the inequality follows from strict incompatibility between P and Q .

Next, we consider the term $\mathbb{E}[R_{emp}(\mathcal{A}(P'); P)]$. Note that P' is drawn uniformly at random from P with replacement, and the number of samples $|P'|$ follows a binomial distribution of $\alpha^{-1}|S|$ trials with probability of success $|P|/|S|$; this distribution has expectation and median $\alpha^{-1}|P|$. By the convexity of $\epsilon(\cdot; \alpha)$ in α , we have that

$$|P|^{-1} \mathbb{E}[R_{emp}(\mathcal{A}(P'); P)] \geq \epsilon(P; \alpha) \quad (16)$$

and similarly for the term in Q . Applying the law of total probability, we find that

$$|S|\epsilon^* > |P|\epsilon(P; \alpha) + |Q|\epsilon(Q; \alpha) \quad (17)$$

Since $|P| + |Q| = |S|$, we have that at least one of $\epsilon(P; \alpha)$ or $\epsilon(Q; \alpha)$ must be less than ϵ^* , which contradicts the optimality of S^* . Thus one of P or Q must be empty.

Finally, we note that by Assumption 4.2, the partition $P = S^* \cap S_P$ and $Q = S^* \cap S_N$ gives an incompatible partition, which yields the result. \square

Remark 1 Lemma 4.1 relies crucially on the incompatibility between the samples from the primary distribution $S_1 \cup \dots \cup S_p$ and the noise distribution $S_{p+1} \cup \dots \cup S_n$ to derive the homogeneity of S^* , a condition which depends on interaction between the data S and the learning algorithm \mathcal{A} . We note that the requirement is empirically satisfied in many data poisoning settings. For example, a common adversary for backdoor attacks against deep neural networks inserts a small synthetic patch in the corner of the image, which, by design, is a location on which the classification does not depend. In this case, the labels for the primary and noise distributions depend on disjoint dimensions of the input, which gives a very clean example of incompatible distributions; given the number of shared (spurious) features, empirical results suggest that the two distributions are, in fact, strictly incompatible for moderately large sets as well.

Remark 2 In general, the larger α is in Assumption 4.2, the easier it is to estimate the value of $\epsilon(S; \alpha)$; the most

convenient case would be for incompatibility to hold even when $\alpha = 1$, in which case $\epsilon(S; \alpha)$ can be evaluated exactly with one call to \mathcal{A} . Unfortunately, for overparameterized models trained using empirical risk minimization, we have that $\epsilon(S; 1) = 0$ for all S (since we assume the problem is realizable in the limit). One method to circumvent this problem is to prevent \mathcal{A} from converging, e.g., by using early stopping. In fact, it is well known that regularizing deep neural networks trained with Stochastic Gradient Descent using early stopping is resilient to noise (Li et al., 2020). In our experiments, we find that combining early stopping with our self-expansion property leads to further improvements in performance.

4.2. Identification using weak learners

The development of the previous section suggests an iterative approach to separating the primary and noise distributions. In particular, if we fix the expansion factor α , at each step, we can identify the set S^* which achieves the lowest expansion error and remove it from the training set. Repeating this procedure partitions the training set into groups of compatible sets. While this suffices to *separate* the primary and noise distributions, it remains to *identify* which components belong to the primary distribution.

In this section, we propose a simplified boosting framework for identification of the primary distribution. We will assume the setting of binary classification and use the 0-1 loss, so that the empirical risk simply counts the number of elements which are misclassified. Our approach is to fit a weak learner to each component, then use each learner to vote on the other components.

Algorithm 1 presents our approach for boosting from homogeneous sets. The subroutine $\text{Loss}_{0,1}$ takes a set of parameters and a set of samples, and returns the empirical zero-one loss over the entire set. Note that votes are weighted by size.

We now turn to characterizing the performance of Algorithm 1. In order for this to succeed, we need an analogous compatibility assumption (cf. Assumption 4.2):

Assumption 4.3 (Compatibility of primary distribution). *Let α be given. Then any pair of (nonempty) sets S_i and S_j drawn from \mathcal{D}_i and \mathcal{D}_j , respectively, such that $i, j \leq n$, are strictly and completely α -compatible.*

Finally, we also require unbiased priors for weak learners:

Assumption 4.4 (Weak learners are unbiased.). *Let S_i be any sets. Then for any untrained weak learner, we have also that $\mathbb{E}[R_{\text{emp}}(\mathcal{A}(\emptyset); S_i)] = |S_i|/2$.*

This condition is necessary in that the weak learners should not be biased toward learning the noise distributions.

Theorem 4.1 (Identification of primary samples). *Let S be a set of samples drawn from a mixture of distribu-*

Algorithm 1 Boosting Homogeneous Sets

Input: Homogeneous sets S_1, \dots, S_N , total number of samples n , number of estimates B , weak learner \mathcal{A}

Output: Votes V_1, \dots, V_N

```

1:  $C_1, \dots, C_N \leftarrow 0$ 
2: for  $i = 1$  to  $N$  do
3:    $V_{i1}, \dots, V_{iN} \leftarrow 0$ 
4:   for  $j = 1$  to  $B$  do
5:      $\theta_{ij} \leftarrow \mathcal{A}(S_i)$ 
6:     for  $k = 1$  to  $N$  do
7:        $V_{ik} \leftarrow V_{ik} + \text{Loss}_{0,1}(\theta_{ij}; S_k)/B$ 
8:     end for
9:   end for
10:  for  $k = 1$  to  $N$  do
11:    if  $V_{ik} > |S_k|/2$  then
12:       $C_k \leftarrow C_k + |S_i|$ 
13:    end if
14:  end for
15: end for
16: for  $i = 1$  to  $N$  do
17:    $V_i \leftarrow C_i > n/2$ 
18: end for
    
```

tions $\{(\alpha_i, \mathcal{D}_i)\}_{i=1}^n$ such that Assumptions 4.2, 4.3, and 4.4 hold, and assume that the ratio of primary samples $p = |S_P|/|S| > 1/2$. Let S_1, \dots, S_N be a partition of S produced by iteratively applying Lemma 4.1. Then if \mathcal{A} is deterministic, Algorithm 1 returns 1 with $B = 1$ for all components containing samples from the primary distribution, and 0 otherwise.

If \mathcal{A} is stochastic, the same result holds with probability

$$[1 - 2 \exp(-2\delta^2 B)]^{MN} \quad (18)$$

where M is the number of primary components, and B is the number of independent weak learners used to fit each primary component.

Proof. We begin with the simple observation that if Assumptions 4.2 and 4.3 hold for S , they also hold for $S \setminus S'$ for any set S' . Thus we are able to apply Lemma 4.1 at each step and so in fact S_1, \dots, S_N are all homogeneous. Additionally, since $p > 1/2$ and a component's vote is weighted by its size, a sufficient condition for success is when all the primary components vote correctly.

We start with the case when \mathcal{A} is deterministic. Let S_i and S_j be a primary component and noise component, respectively. By strict incompatibility, we have that $R_{\text{emp}}(\mathcal{A}(S_i); S_j) > R_{\text{emp}}(\mathcal{A}(\emptyset); S_j) = |S_j|/2$. Thus S_i votes 0 on S_j . Conversely, if S_j is a primary component, then $R_{\text{emp}}(\mathcal{A}(S_i); S_j) < R_{\text{emp}}(\mathcal{A}(\emptyset); S_j) = |S_j|/2$, so S_i votes 1 on S_j . Putting these together and using the fact that

$p > 1/2$, we find that the noise components have weighted vote strictly less than $|S|/2$, while the primary components have weighted vote strictly greater than $|S|/2$, as required.

For the case when \mathcal{A} is stochastic, we apply standard concentration bounds to our estimates of the empirical risk of each component (over the randomness in \mathcal{A}). Let S_i and S_j be a primary and noise component, respectively. Again, strict incompatibility gives $R_{emp}(\mathcal{A}(S_i); S_j) \geq R_{emp}(\mathcal{A}(\emptyset); S_j) + \delta|S_j| = (1/2 + \delta)|S_j|$. Define the sample average empirical risk

$$V_B := \frac{1}{B|S_j|} \sum_{b=1}^B R_{emp}(\mathcal{A}_b(S_i); S_j) \quad (19)$$

computed from B samples over the randomness in \mathcal{A} . Then $\mathbb{E}[V_B] \geq (1/2 + \delta)$ and so by Hoeffding's inequality

$$\Pr[V_B < 1/2] \leq \Pr[|V_B - (1/2 + \delta)| > \delta] \quad (20)$$

$$< 2 \exp(-2\delta^2 B) \quad (21)$$

Thus with probability at least $1 - 2 \exp(-2\delta^2 B)$, primary component S_i votes 0 when S_j is a noise component. By the same argument and using strict compatibility, the bound also holds for S_i voting 1 when S_i and S_j are both from primary components. Putting this together, we recall that a sufficient condition for success of the algorithm occurs when all the primary components vote correctly on all components (both primary and noise), which happens with probability at least

$$[1 - 2 \exp(-2\delta^2 B)]^{MN} \quad (22)$$

as claimed. \square

Remark 3 At a high level, the approach to identifying the primary distribution presented in Lemma 4.1 and Theorem 4.1 follows a simplified boosting framework: at each step, we fit a weak learner to a subset of the distribution, then reweight the remaining training samples by removing the identified component; the ensemble of weak learners is then aggregated using a majority vote. However, our setting is somewhat unique so for clarity we mention several key differences. First, in general the objective of standard boosting is to achieve low population risk, thus the reweighting is performed via more sophisticated methods such as using the empirical loss of the ensemble thus far, e.g., AdaBoost (Freund et al., 1996); in contrast, in our setting there are subpopulations over which we would actually like to maximize the risk. Another difference is that in standard boosting, the ensemble is used during inference to vote on new observations to perform classification, whereas in our algorithm, we use each learner to vote over components of the training set to filter out the noise distributions. Finally, we note that we can succeed with arbitrarily high probability by taking the number of samples B to infinity.

Algorithm 2 Inverse Self-Paced Learning

Input: training set S , total iterations N , annealing schedule $1 \geq \beta_0 \geq \dots \geq \beta_N = \beta_{\min} > 0$, expansion $\alpha \leq 1$, momentum η , incremental learning procedure \mathcal{A} , initial parameters θ_0

Output: $S_N \subseteq S$ such that $|S_N| = \beta_N |S|$

```

1:  $S_0 \leftarrow S$ 
2:  $L \leftarrow \mathbf{0}$ 
3: for  $t = 1$  to  $N$  do
4:    $S' \leftarrow \text{Sample}(S_{t-1}, \alpha)$ 
5:    $\theta_t \leftarrow \mathcal{A}(S', \theta_{t-1})$ 
6:    $L \leftarrow \eta L + (1 - \eta) R_{emp}(\theta_t; S)$ 
7:    $S_t \leftarrow \text{Trim}(L, \beta_t)$ 
8: end for
    
```

5. Inverse self-paced learning

A major question raised by Lemma 4.1 is how to identify the set S^* in its statement. In this section, we propose an algorithm called *Inverse Self-Paced Learning* (ISPL) to solve this problem. Rather than optimizing over all possible subsets of the training data, our objective will instead be to minimize the expansion error over subsets of fixed size $\beta|S|$. The optimization objective is thus defined as follows:

$$S_\beta^* := \arg \min_{S' \subseteq S: |S'| = \beta|S|} \epsilon(S'; \alpha) \quad (23)$$

We attempt to solve for S_β^* by alternating between optimizing parameters θ on the current subset S' , and picking the next subset using the parameters θ . More explicitly, given S' we update θ using a single subset from S' of size $\alpha^{-1}|S'|$. Then we use θ to compute the loss for each element in S , and set S' to be the β fraction of the samples with the lowest losses. To encourage stability of the learning algorithm, the losses are smoothed with an optional momentum term η . We also anneal the parameter β from an initial value β_0 down to the target value β_{\min} in order encourage more global exploration in the initial stages.

Algorithm 2 presents the full algorithm. In addition to the incremental learning procedure \mathcal{A} (e.g., standard SGD), the subroutine `Sample` takes a training set S and returns $\alpha|S|$ elements uniformly at random; while `Trim` takes losses L and returns the $\beta|L|$ samples with the lowest loss.

Finally, we show for certain parameters that Algorithm 2 converges on the following objective over the training set S :

$$F(\theta_t, v_t; \beta_t) := \sum_{i \in S} v_t[i] L(f_{\theta_t}(x_i), y_i) + c \max(0, \beta_t |S| - |v_t|) \quad (24)$$

where v_t is a 0-1 vector, β_t is decreasing, and $L(\cdot, \cdot) \leq c$.

Proposition 5.1. *Let $\alpha = 1$ and $\eta = 0$ in the setting of Algorithm 2, and assume that \mathcal{A} returns the empirical risk minimizer. Then we have that for each round of the algorithm, $F(\theta_t, v_t; \beta_t)$ is decreasing in t and furthermore, $|F(\theta_t, v_t; \beta_t) - F(\theta_{t+1}, v_{t+1}; \beta_{t+1})| \xrightarrow{t \rightarrow \infty} 0$.*

We defer the proof of this statement to the appendix.

Remark 4 When $\alpha = 1$ and $\eta = 0$, we recover vanilla self-paced learning (SPL) with two major differences. First, we start on the full set of samples and train on incrementally smaller sets, while SPL starts with a small set of samples and trains on larger sets. This discrepancy is due to the differing objectives; whereas SPL is a heuristic for converging faster to a global minimizer of the population loss by training first on easy samples, ISPL attempts to converge to a local minimum over a subpopulation. Second, our annealing schedule is defined using the quantile statistics, while SPL uses an absolute loss threshold that generally scales by a multiplicative factor in each iteration. We chose this to counteract the propensity of deep neural networks to suddenly and rapidly interpolate the training data; in our experiments, we found this behavior made the performance of ISPL very sensitive to the specific annealing schedule when using absolute losses. Conversely, in SPL the final threshold is generally set high enough that most (or all) the samples are incorporated by the end, and so the specific schedule may have a smaller impact on the final performance.

6. Experimental Results

We implement our approach to defending against backdoor attacks and evaluate our defense against two types of adversaries. The first is the standard patch-based backdoor attack with dirty labels, where the adversary changes the label of an input and also inserts a small patch. The second is a clean label backdoor attack, where the adversary strongly perturbs the training images before inserting the patch, but does not change the label. Our datasets are standard in the literature. As baselines, we also trained an undefended network on the entire dataset (No defense) and only the clean data (Clean). Full experimental results are given in the appendix.

6.1. Dirty label backdoor scenario

The dirty label backdoor scenario follows the threat model described in Gu et al. (2019). The perturbation function τ simply overlays a small pattern on the image. For evaluation, we use the same dataset (CIFAR-10) and setup for our experiments as Tran et al. (2018). Example pairs of clean and poisoned data are shown in Figure 1.

We report results for the standard settings of ϵ in the literature (5% and 10%), and additionally include a higher



Figure 1. Corresponding poisoned (top) and clean (bottom) images from the CIFAR-10 training set demonstrating the range of trigger varieties used in the dirty label backdoor scenario.

Table 1. Performance on dirty label backdoor scenario for select pairs of CIFAR-10 classes. The numbers in column 1 refer to the standard CIFAR-10 labels (e.g., 0 = airplane, 1 = automobile, etc.). S = source class, T = target class, C = clean accuracy (higher is better), A = targeted misclassification accuracy (lower is better).

S / T	ϵ	No defense		This work		Clean	
		C	A	C	A	C	A
7 / 4	5	90.7	98.4	87.7	0.0	91.0	0.1
	10	90.7	98.0	87.3	1.2	90.8	0.1
	20	90.9	98.2	86.5	0.3	90.9	0.0
8 / 6	5	90.9	98.1	87.8	0.2	91.0	0.0
	10	90.8	99.6	87.2	0.0	90.7	0.0
	20	91.0	99.9	86.9	0.0	91.1	0.1
9 / 2	5	90.9	85.8	87.5	0.0	90.7	0.0
	10	90.6	98.2	87.9	0.0	90.9	0.1
	20	90.8	99.1	86.7	0.2	90.7	0.0

rate (20%) to test our method’s response to larger amounts of poison. Table 1 summarizes our results. We see that a model trained using our approach successfully avoids the backdoor at a small decrease in clean accuracy. The performance is largely stable across values of ϵ , indicating that our approach automatically adapts to different levels of poison.

6.2. Clean label backdoor scenario

We also test our approach on the clean label backdoor adversary introduced by (Turner et al., 2018). Their main observation is that dirty label attacks, while highly effective for naive training, introduce data that is obviously mislabelled to a casual (human) observer. To address this problem, they propose three methods of generating poisoned images that appear plausible to humans. The first interpolates the source image toward the target class in the latent space of a GAN; the second two directly minimize the loss with respect to the target class using Projected Gradient Descent with ℓ_2 and ℓ_∞ bounds (Kurakin et al., 2016; Madry et al., 2017). In all cases, a trigger is then applied to all four corners of the perturbed image. Figure 2 displays examples of images



Figure 2. Corresponding poisoned (top) and clean (bottom) images from the CIFAR-10 training set used in the clean label backdoor scenarios; from left to right, the method used is GAN, ℓ_∞ , ℓ_2 , ℓ_2 .

Table 2. Performance on CIFAR-10, clean label backdoor scenario for select pairs of CIFAR-10 classes. The numbers in column 2 refer to the standard CIFAR-10 labels. M = method, T = target class, C = clean accuracy (higher is better), A = targeted misclassification accuracy (lower is better).

M	T	ϵ	No defense		This work		Clean	
			C	A	C	A	C	A
GAN	0	6	90.6	1.7	87.1	0.0	90.7	0.0
		25	90.7	74.3	87.2	0.4	90.6	0.0
ℓ_∞	2	6	90.4	89.7	87.1	0.1	90.4	0.0
		25	90.0	95.9	87.0	0.6	90.2	0.0
ℓ_2	4	6	90.7	74.4	87.3	0.1	90.4	0.0
		25	90.5	94.6	86.8	4.4	90.4	0.0

from the training sets. We remark that although the images do appear somewhat unnatural, they are not blatantly mislabelled as in the dirty label scenario.

Table 2 presents selected results. Our method successfully defends against the attack in all cases in the 6% scenario; when 25% of the target class is poisoned, the adversary succeeds in installing a backdoor only in a handful of cases, but even in the worst case our defense still succeeds in reducing the backdoor to a 16.4% success rate (compared to over 90% in most cases for an undefended network).

6.3. Third party evaluation on GTSRB

As part of our participation in a funded research program, we submitted our approach to a third party for evaluation on the German Traffic Sign Recognition Benchmark (GTSRB) dataset. Compared with CIFAR-10, the 43 classes in GTSRB are highly imbalanced, ranging from around 250 to upwards of 2000 samples. Hence, one challenge is that the proportion of clean to poisoned data in a class varies greatly, e.g., a small target class may contain close to 50% poisoned samples at the $\epsilon = 10\%$ overall poisoning level. Additionally, as our approach is based on identifying subpopulations, we also risk removing entire classes by mistake.

Table 3. Performance on third-party GTSRB scenarios. C = clean accuracy (higher is better), A = targeted misclassification accuracy (lower is better).

ϵ	Dirty Label		Adversarial Embedding	
	C	A	C	A
0	92.6	-	92.6	-
1	91.8	2.5	91.6	1.5
5	92.4	2.2	89.0	1.7
10	92.2	2.9	90.0	3.3

Table 3 summarizes our results. In addition to maintaining good performance on the dirty label attack with minimal loss in clean accuracy, our approach was also highly resilient to the Adversarial Embedding attack (Tan and Shokri, 2020), a state-of-the-art adversary which has been shown to break three existing defenses (specifically, the spectral signatures, activation clustering, and neuron pruning defenses). The main idea behind the attack is an adaptive adversarial algorithm that minimizes the difference in the latent representations of clean and poisoned data. All three defenses broken by this attack use a similar approach, namely, analyzing the hidden layers of a naive model trained to convergence in order to identify suspicious behavior, suggesting such approaches suffer from a common blind spot; in contrast, the main step of our approach relies on the dynamics of weak learners, which may render an attack based the final representations of a strong learner ineffective.

7. Conclusion

Backdoor data poisoning attacks on deep neural networks are an emerging class of threats in the growing landscape of deployed machine learning applications. Though defenses exist, many of them use a similar pattern of analyzing the activations of a poisoned model, thus making these techniques reliant on the same implicit assumptions.

We introduce an orthogonal approach to defending deep neural networks against backdoor attacks, based on an analysis of a novel self-expansion property in the training data. Under mild compatibility assumptions about the clean and poisoned data, we show that an ensemble of weak learners fit to self-expanding sets successfully removes the poisoned data. In our experiments, this approach succeeds against several existing backdoor attacks, and an independent third party evaluation corroborates our performance. In particular, our method was found to defend against an *adaptive* poisoning adversary that evades several previous state-of-the-art defenses by exploiting a shared weakness. We believe our analysis and techniques thus present a valuable addition to the toolbox for secure deep learning.

References

- Yossi Adi, Carsten Baum, Moustapha Cisse, Benny Pinkas, and Joseph Keshet. Turning your weakness into a strength: Watermarking deep neural networks by backdoor-ing. In *27th {USENIX} Security Symposium ({USENIX} Security 18)*, pages 1615–1631, 2018.
- Maria-Florina Balcan, Avrim Blum, and Ke Yang. Co-training and expansion: Towards bridging theory and practice. 2005.
- Yoshua Bengio, Jérôme Louradour, Ronan Collobert, and Jason Weston. Curriculum learning. In *Proceedings of the 26th annual international conference on machine learning*, pages 41–48, 2009.
- Bryant Chen, Wilka Carvalho, Nathalie Baracaldo, Heiko Ludwig, Benjamin Edwards, Taesung Lee, Ian Molloy, and Biplav Srivastava. Detecting backdoor attacks on deep neural networks by activation clustering. *arXiv preprint arXiv:1811.03728*, 2018.
- Xinyun Chen, Chang Liu, Bo Li, Kimberly Lu, and Dawn Song. Targeted backdoor attacks on deep learning systems using data poisoning. *arXiv preprint arXiv:1712.05526*, 2017.
- Yoav Freund, Robert E Schapire, et al. Experiments with a new boosting algorithm. In *icml*, volume 96, pages 148–156. Citeseer, 1996.
- Alex Graves, Abdel-rahman Mohamed, and Geoffrey Hinton. Speech recognition with deep recurrent neural networks. In *2013 IEEE international conference on acoustics, speech and signal processing*, pages 6645–6649. Ieee, 2013.
- Tianyu Gu, Brendan Dolan-Gavitt, and Siddharth Garg. Badnets: Identifying vulnerabilities in the machine learning model supply chain, 2019.
- Kaiming He, Xiangyu Zhang, Shaoqing Ren, and Jian Sun. Deep residual learning for image recognition. In *Proceedings of the IEEE conference on computer vision and pattern recognition*, pages 770–778, 2016.
- Sebastian Houben, Johannes Stallkamp, Jan Salmen, Marc Schlipfing, and Christian Igel. Detection of traffic signs in real-world images: The German Traffic Sign Detection Benchmark. In *International Joint Conference on Neural Networks*, number 1288, 2013.
- Lu Jiang, Zhengyuan Zhou, Thomas Leung, Li-Jia Li, and Li Fei-Fei. Mentornet: Learning data-driven curriculum for very deep neural networks on corrupted labels. In *International Conference on Machine Learning*, pages 2304–2313. PMLR, 2018.
- Alex Krizhevsky. Learning multiple layers of features from tiny images. Technical report, 2009.
- M Pawan Kumar, Benjamin Packer, and Daphne Koller. Self-paced learning for latent variable models.
- Alexey Kurakin, Ian Goodfellow, and Samy Bengio. Adversarial examples in the physical world. *arXiv preprint arXiv:1607.02533*, 2016.
- Mingchen Li, Mahdi Soltanolkotabi, and Samet Oymak. Gradient descent with early stopping is provably robust to label noise for overparameterized neural networks. In *International Conference on Artificial Intelligence and Statistics*, pages 4313–4324. PMLR, 2020.
- Aleksander Madry, Aleksandar Makelov, Ludwig Schmidt, Dimitris Tsipras, and Adrian Vladu. Towards deep learning models resistant to adversarial attacks, 2017.
- Deyu Meng, Qian Zhao, and Lu Jiang. What objective does self-paced learning indeed optimize?, 2016.
- Philippe Rigollet. Generalization error bounds in semi-supervised classification under the cluster assumption. *Journal of Machine Learning Research*, 8(7), 2007.
- Matthias Seeger. Learning with labeled and unlabeled data. 2000.
- David Silver, Aja Huang, Chris J Maddison, Arthur Guez, Laurent Sifre, George Van Den Driessche, Julian Schrittwieser, Ioannis Antonoglou, Veda Panneershelvam, Marc Lanctot, et al. Mastering the game of go with deep neural networks and tree search. *nature*, 529(7587): 484–489, 2016.
- Aarti Singh, Robert Nowak, and Jerry Zhu. Unlabeled data: Now it helps, now it doesn’t. *Advances in neural information processing systems*, 21:1513–1520, 2008.
- Te Jun Lester Tan and Reza Shokri. Bypassing backdoor detection algorithms in deep learning, 2020.
- Brandon Tran, Jerry Li, and Aleksander Madry. Spectral signatures in backdoor attacks. *arXiv preprint arXiv:1811.00636*, 2018.
- Alexander Turner, Dimitris Tsipras, and Aleksander Madry. Clean-label backdoor attacks. 2018.
- Bolun Wang, Yuanshun Yao, Shawn Shan, Huiying Li, Bimal Viswanath, Haitao Zheng, and Ben Y Zhao. Neural cleanse: Identifying and mitigating backdoor attacks in neural networks. In *2019 IEEE Symposium on Security and Privacy (SP)*, pages 707–723. IEEE, 2019.

Colin Wei, Kendrick Shen, Yining Chen, and Tengyu Ma. Theoretical analysis of self-training with deep networks on unlabeled data. *arXiv preprint arXiv:2010.03622*, 2020.

Xuchao Zhang, Xian Wu, Fanglan Chen, Liang Zhao, and Chang-Tien Lu. Self-paced robust learning for leveraging clean labels in noisy data. In *Proceedings of the AAAI Conference on Artificial Intelligence*, volume 34, pages 6853–6860, 2020.

A. Additional Proofs

We present a proof of the convergence of the Inverse Self Paced Learning algorithm as stated in Proposition 5.1.

Proof. The statement is more or less a direct consequence of the alternating convex minimization strategy. Recall first that since $\alpha = 1$ and $\eta = 0$, Lines 4 and 6 in Algorithm 2 have no effect.

We prove the statement in two steps. First we claim that

$$F(\theta_{t+1}, v_t; \beta_t) \leq F(\theta_t, v_t; \beta_t) \quad (25)$$

Note that v_t in the optimization objective F plays the role of S_t in Algorithm 2. The inequality follows from the optimization on Line 5 in Algorithm 2, which sets θ_{t+1} to the empirical risk minimizer of the set v_t .

Next, we claim that

$$F(\theta_{t+1}, v_{t+1}; \beta_{t+1}) \leq F(\theta_{t+1}, v_t; \beta_t) \quad (26)$$

Since $0 \leq L(\cdot, \cdot) < c$, the optimal size of the set S_t is $|v_t| = \beta_t |S|$. Since β_t is decreasing, we have that $|v_{t+1}| \leq |v_t|$. Thus the number of elements in the trimmed empirical loss is non-increasing (Line 7).

Combining the two inequalities shows that the objective function is decreasing in t . Since $F(\theta_t, v_t; \beta_t)$ is a decreasing sequence bounded from below by zero, the monotone convergence theorem gives the second result. \square

B. Experimental Details

B.1. Defense set up and hyperparameters

For our defense, we use the same set of hyperparameters across all experiments. We run 8 rounds of ISPL, each of which returns a component consisting of roughly 12% of the total samples. Let p be the target percentage of samples over the remaining samples (i.e., $p \approx 1/(8 - i + 1)$ in the i^{th} iteration). Then the number of iterations N is set to $2 + \min(3, 1/p)$. β starts at $3 * p$ in the first iteration, then drops linearly to its final value of p over the next 2 iterations. When trimming the training set, we also additionally include the top $p/8$ samples per class to prevent the network from collapsing to a trivial solution. For the learning procedure \mathcal{A} , we use standard SGD, trained for 2 epochs per iteration. The expansion factor α is set to $1/4$, and the momentum factor η is set to 0.9.

We run ISPL 3 times to generate 24 weak learners. For the boosting framework, each component votes on a per-sample basis. The sample is preserved if the modal vote equals the given label, with ties broken randomly. We also include a self-training step by training a fresh model for 40 epochs on the recovered samples and adding back any rejected samples whose labels agree with the model’s prediction to produce the final dataset.

For CIFAR-10, we use a PreActResNet18 model optimized using vanilla SGD with learning rate 0.02, momentum 0.9, and weight decay $5e-4$. For the final dataset, we train for 100 epochs and drop the learning rate by 10 at 75 and 90 epochs. We report the performance of out of three runs, using the run that achieved the median targeted misclassification accuracy.




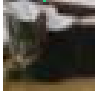
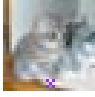



B.2. Dirty label backdoor scenario

Our datasets follow the construction in Tran et al. (2018). Each scenario has a single source and target class. The set of perturbations consists of an L-shape, X-shape, or pixel. For each scenario, a random perturbation shape, color, and position is selected, and an ϵ percentage of the target class is replaced with the perturbed images from the source class (which are relabelled to the target class). The set of (source, target) pairs are (airplane, bird), (automobile, cat), (cat, dog), (horse, deer), (automobile, cat), (ship, frog), (truck, bird), (cat, horse). Table 4 presents results for $\epsilon = 5, 10, 20\%$ and all (source, target) pairs.

B.3. Clean label backdoor scenario

For the clean label backdoor scenario, we use the public datasets provided by Turner et al. (2018). This attack tries to poison the model by creating perturbed examples of the target class, then inserting a trigger without changing the label; the idea is

Table 4. Performance on CIFAR-10, dirty label backdoor scenario. C = clean accuracy (higher is better), A = targeted misclassification accuracy (lower is better).

Source	Target	Image	ϵ	No defense		This work		Clean	
				C	A	C	A	C	A
Airplane	Bird		5	90.7	87.4	87.5	0.1	90.7	0.0
			10	90.8	96.5	87.6	0.0	90.9	0.0
			20	90.7	97.1	87.5	0.3	91.2	0.0
Automobile	Cat		5	90.6	95.4	87.8	0.0	91.1	0.0
			10	90.7	96.4	87.6	0.0	90.8	0.0
			20	91.2	98.4	86.9	0.0	91.2	0.0
Bird	Dog		5	91.0	97.7	87.8	0.0	90.9	0.3
			10	90.7	99.0	86.8	0.5	91.2	0.0
			20	91.0	97.8	86.4	3.4	90.6	0.2
Cat	Dog		5	90.3	0.0	87.5	0.7	91.0	0.0
			10	90.4	4.1	86.5	1.1	90.9	0.0
			20	90.1	79.5	86.2	0.5	90.6	0.0
Cat	Horse		5	90.8	98.3	87.5	0.2	91.0	0.0
			10	91.2	98.2	87.5	0.0	90.6	0.0
			20	90.8	98.7	87.1	0.2	90.9	0.0
Horse	Deer		5	90.7	98.4	87.7	0.0	91.0	0.1
			10	90.7	98.0	87.3	1.2	90.8	0.1
			20	90.9	98.2	86.5	0.3	90.9	0.0
Ship	Frog		5	90.9	98.1	87.8	0.2	91.0	0.0
			10	90.8	99.6	87.2	0.0	90.7	0.0
			20	91.0	99.9	86.9	0.0	91.1	0.1
Truck	Bird		5	90.9	85.8	87.5	0.0	90.7	0.0
			10	90.6	98.2	87.9	0.0	90.9	0.1
			20	90.8	99.1	86.7	0.2	90.7	0.0

that, by making a subpopulation of the target class “harder to classify”, the model will instead learn to associate the trigger with the target class without needing to change any labels. Table 5 presents results from the full dataset. We note that, while there are visual artifacts and inconsistencies in the sample images (Column 3), in general the images are not obviously mislabelled (as in the dirty label scenario).

B.4. Ablation studies

We conduct some additional ablation studies to better understand the effects of the two main hyperparameters in Algorithm 2: the expansion factor α and the subset size β . Computationally, larger β means fewer components and thus fewer outer iterations of ISPL (and is thus more efficient); in our main experiments, we use $\beta = 1/8$ and thus run ISPL 8 times in sequence to generate 8 components. Additionally, as discussed in Remark 2, larger α means better estimates of the expansion error $\epsilon(\cdot; \alpha)$; on the other hand, smaller α is a more stringer requirement, since mixing distributions increases the expansion factor. Therefore we would expect that smaller α leads to better identification of homogeneous components on average, but also less stability in the results.

Tables 6 and 7 present the full results of the ablation studies. Our main finding is that our method is robust to the expansion factor α at $\beta = 1/4$, with smaller α being slightly more effective at identifying poison, at a slight drop in clean accuracy. Additionally, increasing β seems to have little effect in the dirty label scenario, and a detrimental effect in the clean label scenario, particularly when α is larger. This is consistent with the notion that the clean label scenario is more “subtle”, and so when α and β are too large, the components are more likely to converge to a mixed distribution.

Defending Backdoors Using Self-Expansion

Table 5. Performance on CIFAR-10, clean label backdoor scenario. C = clean accuracy (higher is better), A = targeted misclassification accuracy (lower is better).

Method	Target	Image	ϵ	No defense		This work		Clean	
				C	A	C	A	C	A
GAN	Airplane		6	90.6	1.7	87.1	0.0	90.7	0.0
			25	90.7	74.3	87.2	0.4	90.6	0.0
	Bird		6	90.6	45.2	87.5	0.5	90.4	0.0
			25	90.3	78.1	87.2	16.4	90.3	0.1
	Deer		6	90.5	10.7	87.2	0.2	90.6	0.1
			25	90.5	46.3	87.0	1.1	90.2	0.0
	Horse		6	90.4	70.8	87.0	0.1	90.4	0.0
			25	90.5	84.7	87.2	0.5	90.4	0.0
	Truck		6	90.6	51.6	87.0	0.3	90.5	0.0
			25	90.5	67.3	87.4	0.7	91.0	0.2
ℓ_∞	Airplane		6	90.3	81.8	86.8	0.0	90.7	0.0
			25	90.5	93.0	87.0	0.1	90.4	0.0
	Bird		6	90.4	89.7	87.1	0.1	90.4	0.0
			25	90.0	95.9	87.0	0.6	90.2	0.0
	Deer		6	90.5	89.9	87.3	0.2	90.6	0.1
			25	90.2	93.5	86.6	1.2	90.6	0.2
	Horse		6	90.6	89.9	86.7	0.2	90.5	0.0
			25	90.6	94.9	86.9	10.7	90.4	0.0
	Truck		6	90.7	95.3	87.6	0.3	90.7	0.1
			25	90.2	98.4	86.9	1.5	91.0	0.0
ℓ_2	Airplane		6	90.7	23.4	86.9	0.0	90.8	0.0
			25	90.3	82.1	87.3	0.8	90.5	0.0
	Bird		6	90.4	82.0	87.5	0.4	90.5	0.1
			25	90.4	92.4	87.3	2.1	90.9	0.0
	Deer		6	90.7	74.4	87.3	0.1	90.4	0.0
			25	90.5	94.6	86.8	4.4	90.4	0.0
	Horse		6	90.8	45.5	87.4	0.1	90.6	0.0
			25	90.5	89.7	86.9	0.2	90.1	0.0
	Truck		6	90.5	57.6	87.3	0.2	90.8	0.2
			25	90.6	95.8	87.1	9.8	90.3	0.0

Defending Backdoors Using Self-Expansion

Table 6. Performance on dirty label backdoor scenario for select pairs of CIFAR-10 classes. Highlighted cells correspond to the settings used in our main experiments. The numbers in column 1 refer to the standard CIFAR-10 labels (e.g., 0 = airplane, 1 = automobile, etc.). S = source class, T = target class, C = clean accuracy (higher is better), A = targeted misclassification accuracy (lower is better).

S / T	ϵ	$\alpha = 1/16$		$\alpha = 1/8$		$\alpha = 1/4$	
		C	A	C	A	C	A
7 / 4	5	85.8	0.6	87.7	0.0	87.8	0.4
	10	86.3	0.6	87.3	1.2	88.0	0.4
	20	85.7	0.3	86.5	0.3	86.8	0.9
$\beta = 1/4$ 8 / 6	5	86.4	0.0	87.8	0.2	87.5	0.0
	10	86.4	0.0	87.2	0.0	87.7	0.0
	20	86.3	0.1	86.9	0.0	87.5	0.0
9 / 2	5	87.0	0.0	87.5	0.0	87.9	0.0
	10	87.1	0.0	87.9	0.0	87.5	0.0
	20	86.7	0.0	86.7	0.2	87.9	0.0
7 / 4	5	87.2	0.3	86.6	0.2	87.7	0.4
	10	86.0	0.2	86.8	0.3	87.5	3.0
	20	86.1	9.0	87.7	5.0	87.8	8.7
$\beta = 1$ 8 / 6	5	85.7	0.0	87.0	0.1	87.3	0.0
	10	87.4	0.1	87.7	0.0	88.0	0.0
	20	86.6	0.1	86.9	0.0	87.9	0.2
9 / 2	5	86.7	0.0	87.6	0.0	88.0	0.0
	10	87.0	0.0	87.8	0.0	88.2	0.0
	20	86.9	0.0	87.2	0.0	87.6	0.0

Table 7. Performance on CIFAR-10, clean label backdoor scenario for select pairs of CIFAR-10 classes. Highlighted cells correspond to the settings used in our main experiments. The numbers in column 2 refer to the standard CIFAR-10 labels. M = method, T = target class, C = clean accuracy (higher is better), A = targeted misclassification accuracy (lower is better).

M	T	ϵ	$\alpha = 1/16$		$\alpha = 1/8$		$\alpha = 1/4$	
			C	A	C	A	C	A
GAN	0	6	86.1	0.0	87.1	0.0	87.1	0.1
		25	86.6	0.3	87.2	0.4	86.8	9.7
	ℓ_∞	2	6	86.1	1.0	87.1	0.1	87.0
25			85.6	0.5	87.0	0.6	85.7	6.2
ℓ_2	4	6	86.3	0.1	87.3	0.1	86.9	0.3
		25	85.6	5.7	86.8	4.4	86.2	38.9
GAN	0	6	86.2	0.0	87.3	0.0	87.7	0.0
		25	86.6	5.4	86.7	10.1	87.1	17.0
	ℓ_∞	2	6	86.5	0.1	87.5	0.0	87.6
25			85.8	0.1	86.8	28.9	86.6	80.2
ℓ_2	4	6	85.9	0.1	87.0	0.3	87.3	0.2
		25	86.2	31.8	86.6	39.6	87.5	85.9